Inorganic Chemistry

Article

pubs.acs.org/IC

Chemistry of Reduced Monomeric and Dimeric Cobalt Complexes Supported by a PNP Pincer Ligand

Sergio S. Rozenel, Rosa Padilla, and John Arnold*

Department of Chemistry, University of California, Berkeley, California 94720, United States

Supporting Information

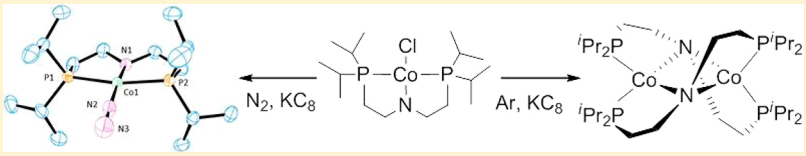

ABSTRACT: The reduction chemistry of cobalt complexes with HPNP (HPNP = $HN(CH_2CH_2P^iPr_2)_2$) as a supporting ligand is described. Reaction of $[(HPNP)CoCl_2]$ (**1**) with *n*-BuLi generated both the deprotonated Co(II) species [(PNP)CoCl] (**2**) along with the Co(I) complex [(HPNP)CoCl] (**3**). Products resulting from reduction of **2** with KC_8 vary depending upon the atmosphere under which the reduction is performed. Monomeric square planar $[(PNP)CoN_2]$ (**4**) is obtained under dinitrogen, whereas dimeric $[(PNP)Co]_2$ (**5**) is formed under argon. Over time, **5** activates a C−H bond in the PNP ligand to form the species $[Co(H)(\mu\text{-PNP})(\mu\text{-}^iPr_2PCH_2CH_2NCHCH_2P^iPr_2)Co]$ (**6**). We also observed the oxidative addition of H−Si bond to complex **3** to form $[(HPNP)CoCl(H)SiH_2Ph]$ (**7**). ^1H NMR studies showed that species **7** is in equilibrium with **3** and silane in solution. Complex **3** can be oxidized with $AgBPh_4$ to generate $\{(HPNP)CoCl\}BPh_4$ (**8**), a square planar species with a formal electron count of 15 electrons.

INTRODUCTION

Cobalt complexes in low oxidation states and low coordination numbers are inherently reactive,[1] being useful for a series of catalytic transformations such as the polymerization of olefins[2] and hydrosilation of 1-hexene.[3] For these types of transformations, the use of multidentate ligands has led to a better understanding of the reactivity at the Co metal center by stabilizing reactive species and potential intermediates. The approach has been used by Holland to isolate 3-coordinate Co complexes with nacnac type ligands,[4] including a tricoordinate Co(I) hydride in a high spin configuration.[5,6] Chirik synthesized a series of anionic, neutral, and cationic Co bis(imino)pyridine species bound to N_2, and showed by density functional theory (DFT) calculations that all the compounds are Co(I) centers with the chelating ligand being reduced.[7] With the $(^tBu_2PCH_2SiMe_2)_2N^-$ ligands, Caulton characterized a 3-coordinate cobalt complex that reversibly binds N_2.[8] Using the ligand $^tBuN^{(-)}SiMe_2N(CH_2CH_2P^iPr_2)_2$ (N_2P_2) our group synthesized the species $[N_2P_2]Co$ and $[N_2P_2]CoH$. The former reacts with aryl azides at low temperatures, generating a species whose reactivity is consistent with an imido Co=NR character.[9,10]

The chemistry of reduced cobalt complexes also includes dimeric and trimeric species. Stuart and co-workers synthesized a Co(I) dimer with a planar Co_2P_2 core capable of coordinating two N_2 molecules, to generate the species $[Co(\mu\text{-}t\text{-}Bu_2P)(PMe_3)(N_2)]_2$, as well as the mixed Co(I)/Co(II) species $[Co_2(\mu\text{-}t\text{-}Bu_2P)_2(PMe_3)_2]$.[11] The trimer $[Cp^*_3Co_3(\mu^2\text{-}H)_3(\mu^3\text{-}H)]$ has also been reported.[12,13] Mindiola and co-workers were able to isolate the $[(N\{2\text{-}P(CHMe_2)_2\text{-}4\text{-}MeC_6H_3\}_2)Co]_2$ dimer, that behaves as a 3-coordinate Co(I) synthon when treated with substrates such as CO or N_2.[1] The Co_2N_2 core in this complex resembles the one observed by Harkins and Peters for related dinuclear Cu(I) systems.[14,15]

Cobalt systems containing a pincer ligand with P and N donor atoms[16−18] have also been successfully applied in a series of catalytic reactions such as ethylene hydrogenation[8] or hydrogenation of alkenes, ketones, aldehydes, and imines.[19,20] Understanding how changes in the ligand environment of such species affects structure and reactivity at the metal center is crucial to efforts to extend the scope of these types of transformations. Of special interest to us is the influence of the amide ligand in the Co reactivity and how its protonation might affect reactivity.[19,20] We have previously shown that the $HN(CH_2CH_2P^iPr_2)_2$ (HPNP) ligand has the potential to stabilize a range of metal species.[21,22] The work described here extends this chemistry to new Co PNP and HPNP complexes in low oxidation states.

RESULTS AND DISCUSSION

The reaction of $[(HPNP)CoCl_2]$ (**1**)[21] with *n*-BuLi produced two complexes: the deprotonated Co(II) species [(PNP)CoCl] (**2**) and the reduced [(HPNP)CoCl] (**3**) (Scheme 1). Complex **2** was obtained as brown crystals from hexane in 42% yield (see Figure 1). The molecular structure, obtained by X-ray crystallography, displays a square planar geometry, with the nitrogen atom on the PNP ligand acting as an amido donor (Co1−N1−C1 and Co1−N1−C9 angles are 124.8(3)° and

Received: July 22, 2013
Published: September 19, 2013

Scheme 1

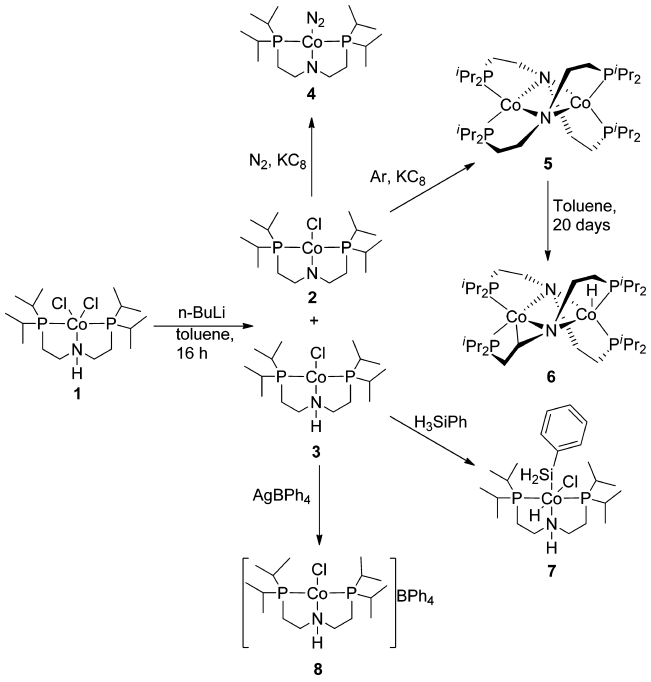

123.9(3)° respectively), and has a magnetic moment consistent with one unpaired electron (μ_{eff} = 1.8 ± 0.2 μ_B).

Compound **3** was crystallized from toluene as blue blocks (18% yield, Figure 1). The X-ray structure shows a metal center in a distorted trigonal pyramidal environment rather than the expected tetrahedral geometry with the N atom in the apical position (τ_4 = 0.84).[23] The N1−Co1−P1, N1−Co1−P2, and N1−Co1−Cl angles are 86.36(4)°, 85.97(4)°, and 110.39(4)°, respectively, and the Co atom is 0.172 Å above the N1−P1−P2 plane.

The N atom of the ligand is sp^3 hybridized, with the Co−N−C angles being 111.1(1)° and 111.7(1)° (Figure 1, Table 1). The magnetic moment observed for **3** is μ_{eff} = 2.6 ± 0.2 μ_B in agreement with a d^8 complex with two unpaired electrons.

When the reduction of **2** with KC_8 was performed under dinitrogen, [(PNP)CoN$_2$] (**4**) was obtained as brown, block-like crystals in 77% yield (Scheme 1). Species **4** is diamagnetic and displays ^{1}H NMR spectroscopic signals expected for the PNP ligand, with the methyl groups appearing as two multiplets (C_{2v} symmetry). A single crystal X-ray analysis of **4** (Figure 2, Table 1) shows a square planar Co, with distances and angles closely related to those observed for **2**. The N−N distance in the dinitrogen ligand (1.124(2) Å) and a strong absorption at 1999 cm^{-1} in the IR spectrum for the N−N stretch indicating only a small degree of activation.[9,22]

Complex **4** is unstable and decomposes in the solid-state in a nitrogen-filled glovebox within weeks, as seen by the disappearance of the signal at 1999 cm^{-1} in the IR (see Supporting Information); we were unable to characterize the decomposition product. Mindiola has observed related behavior and has proposed a Co dimer with bridging N_2 molecules as a pathway for the decomposition.[1]

When the reduction of **2** was performed under argon dimeric [(PNP)Co]$_2$ (**5**) was formed in 50% yield (Scheme 1). Complex **5** crystallizes from diethyl ether with three independent molecules per unit cell, each showing different degrees of disorder in the isopropyl groups, but with almost identical bond distances and angles (Figure 3, Table 2). It displays a Co_2N_2 core similar to that reported by Mindiola[1] with the amido ligand bridging the two metal centers (each one in a distorted tetrahedral environment) and the phosphines of each PNP ligand attached to different Co atoms. In our example, the Co_2N_2 core is bent (Mindiola system is planar), with the Co−N−Co angles close to 74° and the N−Co−Co−N torsion angles in the 125−130° range. The Co−Co distances (2.4220 (5) to 2.4230 (5) Å) are consistent with a single bond between the atoms.[11,24,25] The ^{1}H NMR for **5** is consistent with the proposed structure, showing C_2 symmetry and displaying all the signals for the PNP ligand, with the CH_3 protons of the isopropyl group appearing as four peaks (integrating for 12 H each) and the ^{31}P{^{1}H} NMR showing a broad peak at 85.71 ppm. The magnetic moment of **5** is 0.8 ± 0.1 μ_B/Co, suggesting some antiferromagnetic coupling of the metal centers. The compound was unreactive toward N_2 under the experimental conditions tested: after stirring **5** in toluene for 48 h at room temperature under an N_2 atmosphere, **5** was recovered as the only product.

As observed for **4**, complex **5** rearranges in both the solid state and in solution over time to generate a new species. The ^{1}H NMR spectrum displays broad peaks in the 5 to −2 region and new broad peaks at −6.99 and 11.09 ppm are observed. The ^{31}P{^{1}H} NMR shows three broad signals at 93.5, 86.9, and 72.9 ppm. Based on this data, combined with an X-ray crystallographic analysis, we assign the structure as [Co(H)(μ-PNP)(μ-^{i}Pr$_2$PCH$_2$CH$_2$NCHCH$_2$P^{i}Pr$_2$)Co] (**6**) (Scheme 1), formed, presumably, via oxidative addition of a methylene C−H bond atom across the Co−Co bond (Figure 3; Table 2).

The geometry, distances, and angles observed for **6** are very similar to those found in **5**, except for a contraction of the N1−N2 bond (0.1 Å) and a short Co1−C1 distance (2.024(3) Å).

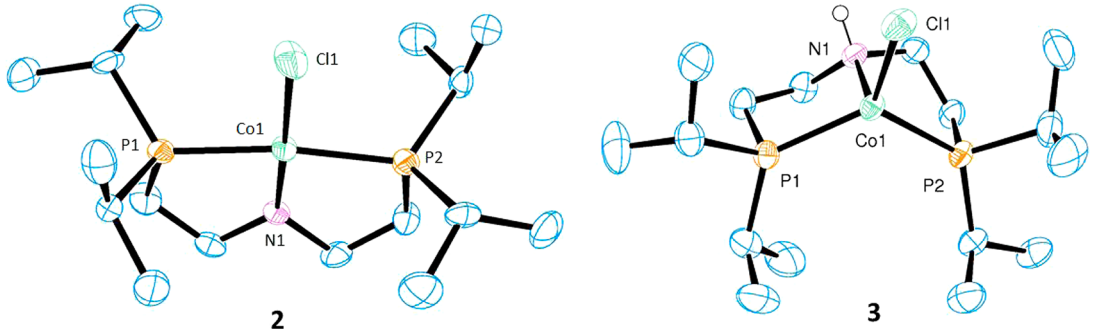

Figure 1. Thermal ellipsoid (50%) plot of **2** and **3**. Hydrogen atoms bound to carbon have been omitted for clarity.

dx.doi.org/10.1021/ic4018882 | Inorg. Chem. 2013, 52, 11544−11550

Table 1. Selected Bond Distances and Angles for Co Complexes 2−4 and 8

	2[a]	3[a]	4[b]	8[a]
Co1−X	2.215(1) Å	2.2566(6) Å	1.740(1) Å	2.1786(9) Å
Co1−P1	2.186(1) Å	2.2550(6) Å	2.1737(4) Å	2.2388(8) Å
Co1−P2	2.201(1) Å	2.2521(6) Å	2.1638(4) Å	2.2390(8) Å
Co1−N1	1.834(4) Å	2.152(2) Å	1.856(1) Å	1.975(2) Å
X−Co1−P1	92.45(5)°	123.54(2)°	95.15(4)°	93.60(3)°
X−Co1−P2	95.32(6)°	116.35(2)°	94.49(4)°	93.95(3)°
X−Co1−N1	178.0(1)°	110.39(4)°	170.55(5)°	178.20(7)°
P1−Co1−P2	171.50(6)°	118.38(2)°	168.54(2)°	172.35(3)°

[a]X = Cl1. [b]X = N2.

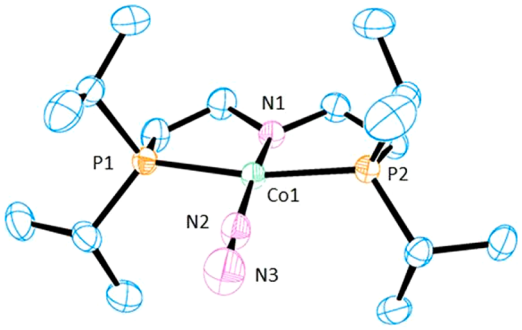

4

Figure 2. Thermal ellipsoid (50%) plot of **4**. Hydrogen atoms have been omitted for clarity.

Table 2. Selected Bond Distances and Angles for Co Complexes 5 and 6

	5	6
Co1−Co2	2.4223(5) Å	2.4151(6) Å
N1−N2	2.943(3) Å	2.824(3) Å
Co1−P1	2.1854(5) Å	2.1772(7) Å
Co1−P2	2.2352(6) Å	2.2174(8) Å
Co1−N1	1.994(2) Å	1.910(2) Å
Co1−N2	2.048(2) Å	2.002(2) Å
Co1−C1	2.833(2) Å	2.024(3) Å
Co2−H101		1.40(3) Å
Co1−N1−Co2	73.60(6)°	74.67(6)°
N1−Co1−N2	93.45(7)°	92.36(7)°
Co1−N2−Co2	73.33(6)°	74.60(6)°
N1−Co2−N2	93.02(7)°	88.38(7)°

For **5**, all the Co−C distances are larger than 2.8 Å. The hydride ligand was located in the Fourier map and refined isotropically with no constraints. The Co1−C1 distance is within the values expected for a Co−C bond (e.g., $[N_2P_2CoCH_3]$: 1.995(5) Å, $[N_2P_2CoCH_2Si(CH_3)_3]$: 2.033(2) Å).[26] The Co−H distance (1.40(3) Å) is in agreement with related Co−H complexes.[26,27] Further evidence for the presence of a hydride was found upon treatment of the complex with CCl_4 in C_6D_6, whereupon the latter signal disappeared and a new peak corresponding to the formation of $CHCl_3$ was observed. Related C−H cyclometalations have been

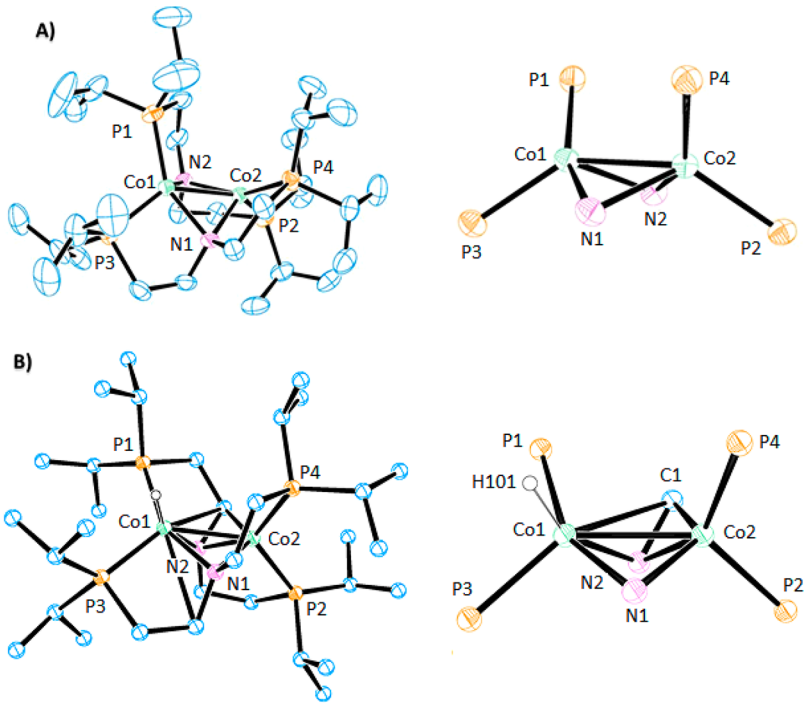

Figure 3. Right: Thermal ellipsoid (50%) plot of **5** (A) and **6** (B) with hydrogen bound to carbon omitted for clarity. Left: Thermal ellipsoid (50%) plot of **5** (A) and **6** (B) Co_2N_2 cores.

dx.doi.org/10.1021/ic4018882 | *Inorg. Chem.* 2013, 52, 11544−11550

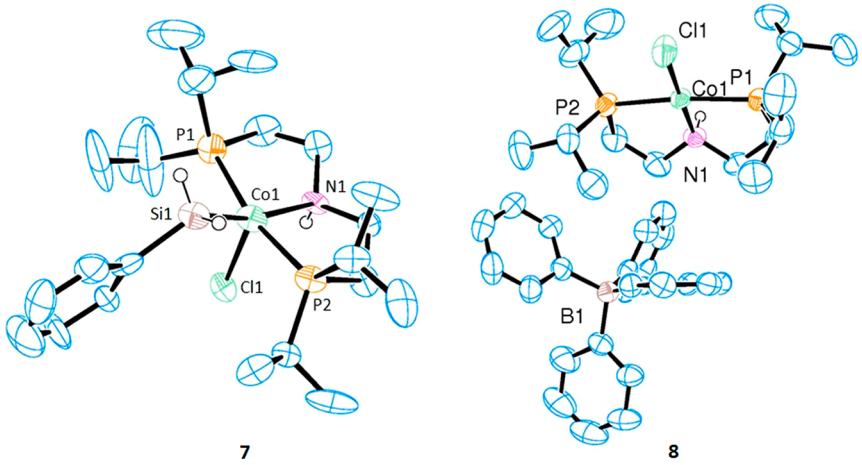

Figure 4. Thermal ellipsoid (50%) plot of **7** and **8**. Hydrogen atoms bound to carbon have been omitted for clarity.

reported by Schneider et al.[28] and Chirik et al.[29] for monomeric species.

To gain insights about the formation of **4** and **5**, as well as the transformation of **5** into **6**, DFT calculations were performed using the pure DFT function TPSS.[30,31] Complexes $\mathbf{4}^{Me}$, $\mathbf{5}^{Me}$, and $\mathbf{6}^{Me}$ (where the isopropyl groups were replaced by methyl groups) were modeled. In the case of $\mathbf{5}^{Me}$ and $\mathbf{6}^{Me}$ the singlet, triplet, and quintuplet electronic states were calculated. For complex $\mathbf{5}^{Me}$, the results showed that the singlet electronic state is more stable by 1.9 kcal/mol than the triplet electronic configuration; however, the singlet state displays an almost planar conformation of the Co_2N_2 core, while the triplet electronic state accurately describes the angles and distances observed experimentally (See Supporting Information). The quintuplet electronic state is higher in energy (15.6 kcal/mol) and displays a planar conformation at the Co_2N_2 core. For $\mathbf{6}^{Me}$, the singlet electronic state is the lowest in energy by 18.2 kcal/mol (in comparison with the triplet) and is a good fit to the experimental data (See Supporting Information). The calculations show that the formation of two molecules of complex $\mathbf{4}^{Me}$ is favored over the formation of complex $\mathbf{5}^{Me}$ by 12 kcal/mol. The oxidative addition of the C−H bond in $\mathbf{5}^{Me}$ to generate $\mathbf{6}^{Me}$ is downhill by 11 kcal/mol. These results are in agreement with the experimental observations.

The reactivity and stability of the HPNP−Co(I) complex **3** is different than that seen for the PNP species **4** and **5**. Complex **3** is stable in solid state and in solution and it can participate in both 1- and 2-electron oxidation processes. For example, reaction of **3** with H_3SiPh in toluene produces [(HPNP)CoCl-(H)SiH_2Ph] (**7**), formed by the oxidative addition of a H−Si bond to the cobalt metal center. Complex **7** is diamagnetic, and the resonances for the HPNP ligand and the silane were found in the ^{1}H NMR spectrum. The SiH_2 protons appeared as a singlet at 4.69 ppm, while the Co−H peak was observed as triplet at −28.78 ppm (J_{P-H} 56 Hz). An X-ray diffraction study of **7** showed two independent molecules per unit cell. Poor data and twinning problems did not allow us to refine the structure to acceptable values (Figure 4, Table 1), but the study displayed the cobalt metal center in a square pyramidal environment (the hydride ligand was not located), with the silane ligand *trans* to the amine.

Interestingly, we discovered that complex **7** is in equilibrium in solution with **3** and free silane. Since **3** is blue while **7** is yellow, we were able to probe this process using UV−vis spectroscopy. A van't Hoff analysis of the data between 60 °C−90 °C showed that, as expected, the reaction is enthalpically driven with $\Delta H° = -19.9 \pm 1.3$ kcal/mol overcoming the large, negative entropy ($\Delta S° = -46 \pm 3$ cal/mol) (see Supporting Information).

Protonation of the PNP ligand also affects the coordination mode and stability of the Co(II) species. Attempts to abstract the chloride ligand in **3** were unsuccessful; however, the compound readily loses an electron on treatment with $AgBPh_4$ in tetrahydrofuran (THF) to generate {(HPNP)CoCl}BPh_4 (**8**) in 78% yield (Scheme 1). While [(HPNP)$CoCl_2$] (**1**) is trigonal bipyramidal, complex **8** displays a square planar geometry, with angles and distances in close agreement with those found in **2** (Figure 4, Table 1). The N−Co distance showed an elongation of 0.14 Å due the inability of the amine ligand to donate the lone pair to the metal center; angles around the N ligand are in accord with sp^3 hybridization. With a formal electron count of 15 electrons, complex **8** might be expected to be highly reactive: thus far we have only observed that it decomposes in the solid state within weeks to generate low yields of **1** along with unidentified products.

CONCLUSIONS

Our findings add to the growing body of work that shows that pincer ligand systems can act as versatile supporting scaffolds in transition metal chemistry. Specifically, the PNP moiety provides access to a range of reduced Co complexes in which the form of the ligand (anionic amide vs neutral amine) and the atmosphere (dinitrogen vs argon) used in the synthesis of the reduced species play substantial roles in determining reaction outcomes. The HPNP complex **3** is formed by reduction of **1** with *n*-BuLi, while the PNP−monomeric, square-planar N_2 complex **4** is obtained when **2** is reduced in N_2 atmosphere. The dimeric PNP species **5** is formed when **2** is reduced under Ar, and it displays a distorted tetrahedral environment with the PNP ligand bridging the two metal centers via the nitrogen atom. For **3**, we observed oxidative addition of H−Si bonds and 1-el oxidation, forming **7** and the 15-el complex **8**, respectively. Compounds **4**, **5**, and **7** are unstable and decompose over time in solid-state and in solution. Complex **5** undergoes intramolecular C−H activation of the PNP ligand to form **6**, where the hydride and the CH moieties are attached to different metal centers. DFT calculations are in agreement with these experimental findings: formation of two molecules of **4** is

dx.doi.org/10.1021/ic4018882 | *Inorg. Chem.* 2013, 52, 11544−11550

thermodynamically favored over the formation of the dimeric species **5** by 12 kcal/mol, and the C−H bond activation in **5** to generate **6** is 11 kcal/mol downhill.

EXPERIMENTAL SECTION

General Considerations. Unless otherwise noted, all reactions were performed using standard Schlenk techniques under a N_2-atmosphere or in a N_2-atmosphere glovebox. Solvents were dried by passing through a column of activated alumina and degassed with nitrogen.[32] C_6D_6 and $C_6D_5CD_3$ were dried over Na/benzophenone and vacuum transferred. All NMR spectra were obtained in C_6D_6 (at ambient temperature) or $C_6D_5CD_3$ (for low temperature experiments) using Bruker AVQ-400, AV-500, or AV-600 spectrometers. ^{1}H NMR chemical shifts (δ) were calibrated relative to the residual solvent peak. Magnetic susceptibility measurements were performed in C_6D_6 according to the Evans NMR method.[33] Melting points were determined using sealed capillaries prepared under a nitrogen atmosphere. Infrared (IR) spectra were recorded with a Thermo Scientific Nicolet iS10 series FTIR spectrophotometer as a powder or a Nujol mull between KBr plates. Elemental analyses were performed at the University of California, Berkeley Microanalytical Facility. X-ray crystal diffraction analyses were performed at the University of California, Berkeley CHEXRAY facility. [(HPNP)$CoCl_2$] (**1**) was prepared according to literature procedure.[21] The remaining starting materials were obtained from Aldrich and used without further purification.

*[(PNP)CoCl] (**2**).* A 1.6 M solution of *n*-BuLi (0.90 mL, 1.4 mmol) in hexanes was added to a suspension of [(HPNP)$CoCl_2$] (0.60 g, 1.4 mmol) in 25 mL of toluene at −78 °C. The suspension immediately turned from purple to red. The reaction mixture was allowed to warm to room temperature and was stirred for 3 h. The solvent was removed under vacuum, and the product was extracted with hexanes (3 × 15 mL). The solution was concentrated and cooled to −40 °C to give brown, block-like crystals (0.23 g, 42%). Crystals suitable for an X-ray diffraction study were grown from a concentrated solution of diethyl ether cooled to −40 °C. ^{1}H NMR (C_6D_6, 25 °C, 400 MHz): δ 1.73 (br), 1.06 (br), 0.31 (br), −3.47 (br), −17.32 (br). ^{31}P{^{1}H} NMR (C_6D_6, 25 °C, 400 MHz): δ −1.83 (br). IR (cm^{-1}) 2816 (m), 2797 (s), 2708 (w), 2625 (w), 1404 (w), 1364 (s), 1318 (m), 1238 (s), 1208 (m), 1098 (s), 1024 (s), 882 (m), 723 (s), 632 (s). Anal. Calc: C, 48.19; H, 9.10; N, 3.51. Observed C, 48.17; H, 9.48; N, 3.50. Mp 60−63 °C. μ_{eff} = 1.8 ± 0.2 μ_B.

*[(HPNP)CoCl] (**3**).* After the extraction of **2**, the remaining residue was extracted with toluene (4 × 15 mL) to give a blue solution. The solution was concentrated and cooled to −40 °C to give blue, block-like crystals (0.10 g, 18%). Crystals suitable for an X-ray diffraction study were grown from a concentrated solution of toluene cooled to −40 °C. ^{1}H NMR (C_6D_6, 25 °C, 400 MHz): δ 64.76 (br), 29.22 (br), 20.10 (br), 17.84 (br), 11.70 (br), 10,26 (br), −0.20 (br), −1.76 (br), −13.57 (br). ^{31}P{^{1}H} NMR (C_6D_6, 25 °C, 400 MHz): δ 83.0 (br). IR (cm^{-1}) 3216 (s, N-H), 1408 (w), 1363 (s), 1244 (m), 1181 (m), 1157 (w), 1080 (s), 1044 (s), 1012 (s), 886 (m), 815 (s), 769 (m). 678 (s), 630 (m), 606 (s). Anal. Calc: C, 48.07; H, 9.33; N, 3.50. Observed C, 48.15; H, 9.48; N, 3.59. Mp 186−188 °C. μ_{eff} = 2.6 ± 0.2 μ_B.

*[(PNP)CoN_2] (**4**).* A solution of **2** (0.70 g, 1.8 mmol) in 15 mL of THF was added to a suspension of KC_8 (0.31 g, 2.3 mmol) in 10 mL of THF at −78 °C under an N_2 atmosphere. The suspension immediately turned from brown to red-brown. The reaction mixture was allowed to warm to room temperature and was stirred for 2 h. The solvent was removed under vacuum, and the product was extracted with hexane (3 × 15 mL). The solution was concentrated and cooled to −40 °C to give brown, block-like crystals (0.53 g, 77%). Crystals suitable for an X-ray diffraction study were grown from a concentrated solution of hexane cooled to −40 °C. ^{1}H NMR (C_6D_6, 25 °C, 400 MHz): δ 2.98 (br, 4H, N-*H*), 2.11 (br, 4H, PC*H*(CH_3)$_2$), 1.67 (br, 4H, PCH_2), 1.39 (br, 12H, CH_3), 1.15 (br, 12H, CH_3). ^{31}P{^{1}H} NMR (C_6D_6, 25 °C, 400 MHz): δ 92.54 (s). ^{13}C{^{1}H} NMR (C_6D_6, 25 °C, 400 MHz): δ 61.4 (m, NCH_2), 25.2 (m, PCH(CH_3)), 23.7 (m, PCH_2), 20.0 (s, CH_3), 18.6 (s, CH_3). IR (cm^{-1}) 2816 (m), 2783 (w), 2699 (m), 2621 (w), 1999 (s, N−N), 1402 (w), 1362 (s), 1317 (m), 1234 (s), 1206 (s), 1101 (s), 1065 (m), 1022 (s), 965 (m), 882 (m), 818 (s), 721 (s), 631 (s). Anal. Calc: C, 49.10; H, 9.27; N, 10.74. Observed C, 48.94; H, 9.19; N, 7.79. Complex **4** readily loses N_2. Mp 148−150 °C.

*[(PNP)Co]$_2$ (**5**).* The synthesis was carried out analogously to that of **4** under an Ar atmosphere, starting with KC_8 (0.30 g, 2.2 mmol) and [(PNP)CoCl] (0.75 g, 1.9 mmol), to yield brown, block-like crystals (0.34 g, 50%) after crystallization from hexane. Crystals suitable for an X-ray diffraction study were grown from a concentrated solution of diethyl ether cooled to −40 °C. ^{1}H NMR (C_6D_6, 25 °C, 400 MHz): δ 4.87 (br, 4H, PC*H*(CH_3)), 3.10 (br, 4H, NCH_2), 2.76 (br, 4H, NCH_2), 2.24 (br, 12H, PC*H*(CH_3) (4H) and PCH_2 (8H)), 1.90 (br, 12H, CH_3), 1.31 (br, 12H, CH_3), 0.89 (br, 12H, CH_3), 0.31 (br, 12H, CH_3). ^{31}P{^{1}H} NMR (C_6D_6, 25 °C, 400 MHz): δ 85.71 (br). IR (cm^{-1}) 1260 (s), 1149(w), 1092 (s), 1025 (s), 880 (w), 799 (s), 668 (w), 607 (m). Anal. Calc: C, 52.89; H, 9.99; N, 3.85. Observed C, 52.87; H, 9.66; N, 3.90. Mp 113−116 °C. μ_{eff} = 0.8 ± 0.1 μ_B/Co. MS 726.3325 (M^+).

*[Co(H)(μ-PNP)(μ-PCH_2CH_2NCHCH_2P)Co] (**6**).* **6** is formed by rearrangement of **5** in solution (20 days) and in solid state (two months). ^{1}H NMR (C_6D_6, 25 °C, 400 MHz): δ 11.09 (br), 4.74 (br), 3.11 (br), 2.79 (br), 2.14 (br), 1.85 (br, 1.56 (br), 1.33 (br), 1.02 (br), 0.34 (br), −0.90 (br), −1.49 (br), −6.99 (br, Co-H).). ^{31}P{^{1}H} NMR (C_6D_6, 25 °C, 400 MHz): δ 93.5 (br), 86.9 (br), 72.9 (br). μ_{eff} = 1.2 ± 0.3 μ_B/Co.

*[(HPNP)CoCl(H)SiH_2Ph] (**7**).* H_3SiPh (0.30 mL, 2.4 mmol) was added via syringe to a solution of [(HPNP)CoCl] (0.30 g, 0.75 mmol) in 5 mL of toluene at room temperature. The solution was stirred for 1 h. A color change from blue to yellow was observed. The solution was cooled to −40 °C to give yellow, rod-like crystals (0.25 g, 66%). Crystals suitable for an X-ray diffraction study were grown from a concentrated solution of toluene cooled to −40 °C. ^{1}H NMR ($C_6D_5CD_3$, 25 °C, 400 MHz): δ 8.25 (d, 2H, *o*-C_6H_5), 7.21 (m, 3H, *m*-C_6H_5 and *p*-C_6H_5), 6.20 (br, 1H, N*H*), 4.69 (s, 2H, SiH_2), 2.87 (br, 2H, NCH_2), 2.64 (br, 2H, NCH_2), 2.11 (br, 4H, PC*H*(CH_3)$_2$), 1.61 (br, 4H, PCH_2), 1.25−0.70 (m, 24H, CH_3), −28.78 (m, 1H, Co-H, J_{H-P}: 55 Hz). ^{31}P{^{1}H} NMR ($C_6D_5CD_3$, 25 °C, 400 MHz): δ 87.42 (br), 66.16 (br). IR (cm^{-1}) 3179 (w), 2037 (w), 1260 (s), 1084 (s), 1019 (s), 936 (w), 843 (m), 799 (s), 724 (w), 698 (w). Anal. Calc: C, 52.01; H, 8.93; N, 2.76. Observed C, 51.82; H, 9.11; N, 2.68. Mp 87−91 °C (d).

*[(HPNP)CoCl](BPh_4) (**8**).* A suspension of $AgBPh_4$ (0.22 mL, 0.52 mmol) in 15 mL of THF was added via cannula to a solution of [(HPNP)CoCl] (0.20 g, 0.50 mmol) in 10 mL of THF at room temperature. The reaction mixture turned from a blue solution to a red suspension and the formation of Ag^0 is observed. After stirring for 1 h, the solvent was removed under vacuum, and the product was extracted with THF (3 × 10 mL). The solution was concentrated and cooled to −40 °C to give red, block-like crystals (0.28 g, 78%). Crystals suitable for an X-ray diffraction study were grown from a concentrated solution of THF/diethyl ether cooled to −40 °C. ^{1}H NMR (C_6D_6, 25 °C, 400 MHz): δ 6.23 (br), 5.05 (br), 3.62 (br), 1.48 (br), 0.96 (br), 0.38 (br). IR (cm^{-1}) 3182 (w), 1578 (m), 1424 (m), 1260 (s), 1085 (s), 1031 (s), 800 (s), 732 (s), 705 (s), 612 (m). Anal. Calc: C, 66.82; H, 7.99; N, 1.95. Observed C, 66.81; H, 8.16; N, 1.76. Mp 117−119 °C.

Equilibrium constant measurements by UV−vis for *3*/*7*: Two solutions of known concentration of **3** and phenylsilane were prepared: (a) [**3**] = 0.006 M, [H_3SiPh] = 0.006 M; (b) [**3**] = 0.011 M, [H_3SiPh] = 0.026 M. The solutions were placed in a 1 cm Schlenk-type quartz cell and transferred to Cary 50 UV−vis spectrophotometer adapted with a calibrated liquid nitrogen low-temperature apparatus. The values were recorded each 5 °C in the 60−90 °C temperature range, waiting at least 5 min once the target temperature was reached to ensure equilibrium. The equilibrium constant was calculated by the formula K = [**7**]/([**3**][H_3SiPh]) (where [H_3SiPh] = [H_3SiPh]$_{initial}$ − [**7**]; and [**7**] = [**3**]$_{initial}$ − [**3**]). A Van't Hoff plot was generated for each solution and fitted to a line by the least-squares method. The obtained values were averaged to obtain the thermodynamic parameters.

dx.doi.org/10.1021/ic4018882 | *Inorg. Chem.* 2013, 52, 11544−11550

Crystallographic Analyses. Single crystals of **2**−**8** were coated in Paratone-N oil, mounted on a Kaptan loop, transferred to a Bruker SMART APEX or APEX II QUAZAR diffractometer with CCD area detector,[34] centered in the beam, and cooled by a nitrogen flow low-temperature apparatus that has been previously calibrated by a thermocouple placed at the same position as the crystal. Preliminary orientation matrices and cell constants were determined by collection of 60 10-s frames, followed by spot integration and least-squares refinement. A data collection strategy was computed with COSMO to ensure a redundant and complete data set, and the raw data were integrated using SAINT.[35] The data were corrected for Lorentz and polarization effects, but no correction for crystal decay was applied. An empirical absorption correction based on comparison of redundant and equivalent reflections was applied using SADABS.[36] XPREP[37] was used to determine the space group. The structures were solved using SIR-97[38] and refined on all data by full-matrix least-squares with SHELXL-97.[39] Thermal parameters for all non-hydrogen atoms were refined anisotropically. ORTEP diagrams were created using ORTEP-32.[40]

Computational Details. All structures and energies were calculated using the Gaussian09 suite of programs.[30] Self-consistent field computations were performed with tight convergence criteria on ultrafine grids, while geometry optimizations were converged to tight geometric convergence criteria for all compounds. Spin expectation values $\langle S \rangle^2$ indicated that spin contamination was not significant in any case. Frequencies were calculated analytically at 298.15 K and 1 atm. Structures were considered true minima if they did not exhibit imaginary vibration modes. Optimized geometries were compared using the sum of their electronic and zero-point energies. To reduce the computational time, the isopropyl groups attached to phosphorus were substituted for methyl groups for **4**, **5**, and **6**. The TPSS functional was used to calculate $\mathbf{4}^{Me}$, $\mathbf{5}^{Me}$, and $\mathbf{6}^{Me}$.[30] For geometry optimizations and frequency calculations all atoms were treated with 6-31++G(d,p) basis set.[30] A 5d diffusional function was used for all atoms except H, and no polarization functions were added for H.

■ ASSOCIATED CONTENT

Supporting Information

Relevant experimental and DFT computational data. This material is available free of charge via the Internet at http://pubs.acs.org.

■ AUTHOR INFORMATION

Corresponding Author

*E-mail: arnold@berkeley.edu.

Notes

The authors declare no competing financial interest.

■ ACKNOWLEDGMENTS

We thank the National Science Foundation for funding (Grant CHE-0848931), Drs. A. DiPasquale, and C. Canlas for experimental assistance, and Ashleigh Ward, Daniel Kellenberger, and Thomas Gianetti for helpful discussions. Fellowship support from UC-MEXUS (R.P.) is appreciated.

■ REFERENCES

(1) Fout, A. R.; Basuli, F.; Fan, H. J.; Tomaszewski, J.; Huffman, J. C.; Baik, M. H.; Mindiola, D. J. *Angew. Chem., Int. Ed.* **2006**, *45*, 3291−3295.

(2) Gibson, V. C.; Spitzmesser, S. K. *Chem. Rev.* **2003**, *103*, 283−315.

(3) Brookhart, M.; Grant, B. E. *J. Am. Chem. Soc.* **1993**, *115*, 2151−2156.

(4) Holland, P. L.; Cundari, T. R.; Perez, L. L.; Eckert, N. A.; Lachicotte, R. J. *J. Am. Chem. Soc.* **2002**, *124*, 14416−14424.

(5) Ding, K. Y.; Brennessel, W. W.; Holland, P. L. *J. Am. Chem. Soc.* **2009**, *131*, 10804−10805.

(6) Ding, K. Y.; Pierpont, A. W.; Brennessel, W. W.; Lukat-Rodgers, G.; Rodgers, K. R.; Cundari, T. R.; Bill, E.; Holland, P. L. *J. Am. Chem. Soc.* **2009**, *131*, 9471−9472.

(7) Bowman, A. C.; Milsmann, C.; Atienza, C. C. H.; Lobkovsky, E.; Wieghardt, K.; Chirik, P. J. *J. Am. Chem. Soc.* **2010**, *132*, 1676−1684.

(8) Ingleson, M.; Fan, H. J.; Pink, M.; Tomaszewski, J.; Caulton, K. G. *J. Am. Chem. Soc.* **2006**, *128*, 1804−1805.

(9) Chomitz, W. A.; Arnold, J. *Chem. Commun.* **2008**, 3648−3650.

(10) Chomitz, W. A.; Mickenberg, S. F.; Arnold, J. *Inorg. Chem.* **2008**, *47*, 373−380.

(11) Jones, R. A.; Stuart, A. L.; Atwood, J. L.; Hunter, W. E. *Organometallics* **1983**, *2*, 1437−1441.

(12) Kersten, J. L.; Rheingold, A. L.; Theopold, K. H.; Casey, C. P.; Widenhoefer, R. A.; Hop, C. *Angew. Chem., Int. Ed.* **1992**, *31*, 1341−1343.

(13) Casey, C. P.; Hallenbeck, S. L.; Widenhoefer, R. A. *J. Am. Chem. Soc.* **1995**, *117*, 4607−4622.

(14) Harkins, S. B.; Peters, J. C. *J. Am. Chem. Soc.* **2005**, *127*, 2030−2031.

(15) Mankad, N. P.; Rivard, E.; Harkins, S. B.; Peters, J. C. *J. Am. Chem. Soc.* **2005**, *127*, 16032−16033.

(16) Fryzuk, M. D.; Macneil, P. A. *J. Am. Chem. Soc.* **1981**, *103*, 3592−3593.

(17) Danopoulos, A. A.; Edwards, P. G. *Polyhedron.* **1989**, *8*, 1339−1344.

(18) Danopoulos, A. A.; Edwards, P. G.; Parry, J. S.; Wills, A. R. *Polyhedron.* **1989**, *8*, 1767−1769.

(19) Zhang, G.; Vasudevan, K. V.; Scott, V. L.; Hanson, S. K. *J. Am. Chem. Soc.* **2013**, *135*, 8668−8681.

(20) Zhang, G. Q.; Scott, B. L.; Hanson, S. K. *Angew. Chem., Int. Ed.* **2012**, *51*, 12102−12106.

(21) Rozenel, S. S.; Kerr, J. B.; Arnold, J. *Dalton Trans.* **2011**, *40*, 10397−10405.

(22) Rozenel, S. S.; Arnold, J. *Inorg. Chem.* **2012**, *51*, 9730−9739.

(23) Yang, L.; Powell, D. R.; Houser, R. P. *Dalton Trans.* **2007**, 955−964 ; $\tau^4 = [360° - (\alpha + \beta)]/141°$.

(24) Pauling, L. *Proc. Natl. Acad. Sci. U.S.A.* **1976**, *73*, 4290−4293.

(25) Harley, A. D.; Guskey, G. J.; Geoffroy, G. L. *Organometallics* **1983**, *2*, 53−59.

(26) Chomitz, W. A.; Arnold, J. *Inorg. Chem.* **2009**, *48*, 3274−3286.

(27) Mock, M. T.; Potter, R. G.; O'Hagan, M. J.; Camaioni, D. M.; Dougherty, W. G.; Kassel, W. S.; DuBois, D. L. *Inorg. Chem.* **2011**, *50*, 11914−11928.

(28) Kass, M.; Friedrich, A.; Drees, M.; Schneider, S. *Angew. Chem., Int. Ed.* **2009**, *48*, 905−907.

(29) Atienza, C. C. H.; Bowman, A. C.; Lobkovsky, E.; Chirik, P. J. *J. Am. Chem. Soc.* **2010**, *132*, 16343−16345.

(30) Frisch, M. J.; Trucks, G. W.; Schlegel, H. B.; Scuseria, G. E.; Robb, M. A.; Cheeseman, J. R.; Scalmani, G. B., V.; Mennucci, B.; Petersson, G. A.; Nakatsuji, H.; Caricato, M.; Li, X.; Hratchian, H. P.; Izmaylov, A. F.; Bloino, J.; Zheng, G.; Sonnenberg, J. L.; Hada, M.; Ehara, M.; Toyota, K.; Fukuda, R.; Hasegawa, J.; Ishida, M.; Nakajima, T.; Honda, Y.; Kitao, O.; Nakai, H.; Vreven, T.; Montgomery, J. A.; Peralta, J. E.; Ogliaro, F.; Bearpark, M.; Heyd, J. J.; Brothers, E. K.; Kudin, K. N.; Staroverov, V. N.; Kobayashi, R.; Normand, J.; Raghavachari, K.; Rendell, A. B.; Burant, J. C.; Iyengar, S. S.; Tomasi, J.; Cossi, M.; Rega, N.; Millam, J. M.; Klene, M.; Knox, J. E.; Cross, J. B.; Bakken, V.; Adamo, C.; Jaramillo, J.; Gomperts, R.; Stratmann, R. E.; Yazyev, O.; Austin, A. J.; Cammi, R.; Pomelli, C.; Ochterski, J. W.; Martin, R. L.; Morokuma, K.; Zakrzewski, V. G.; Voth, G. A.; Salvador, P.; Dannenberg, J. J.; Dapprich, S.; Daniels, A. D.; Farkas, Ö.; Foresman, J. B.; Ortiz, J. V.; Cioslowski, J.; Fox, D. J. *Gaussian09*, Revision B.01; Gaussian, Inc.: Wallingford, CT, 2010.

(31) Hebden, T. J.; St. John, A. J.; Gusev, D. G.; Kaminsky, W.; Goldberg, K. I.; Heinekey, D. M. *Angew. Chem., Int. Ed.* **2011**, *50*, 1873−1876.

(32) Alaimo, P. J.; Peters, D. W.; Arnold, J.; Bergman, R. G. *J. Chem. Educ.* **2001**, *78*, 64−64.

(33) Piguet, C. *J. Chem. Educ.* **1997**, *74*, 815−816.

(34) *SMART Area-Detector Software Package*; Bruker Analytical X-ray Systems, Inc.: Madison, WI, 2001−2003.
(35) *SAINT, SAX Area-Detector Integration Program*, V6.40; Bruker Analytical X-ray Systems Inc.: Madison, WI, 2003.
(36) *SADABS Bruker-Nonius Area Detector Scaling and Absorption*, v. 2.05; Bruker Analytical X-ray Systems, Inc.: Madison, WI, 2003.
(37) *PREP (v 6.12) Part of the SHELXTL Crystal Structure Determination Package*; Bruker Analytical X-ray Systems, Inc.: Madison, WI, 2001.
(38) Sheldrick, G. M. *Acta Crystallogr., Sect. A.* **2008**, *64*, 112−122.
(39) *SHELXS Program for the Refinement of X-ray Crystal Structures, Part of the SHELXTL Crystal Structure Determination Package*; Bruker Analytical X-ray Systems Inc.: Madison, WI, 1995−1999.
(40) Farrugia, L. *J. Appl. Crystallogr.* **1997**, *30*, 565.